A Unified Framework for Precoding and Pilot Design for FDD Symbol-Level Precoding

Jianjun Zhang, *Member, IEEE*, and Christos Masouros, *Senior Member, IEEE*

***Abstract*—Large-scale antenna array techniques are key enablers for modern wireless communication systems. Channel state information (CSI) is indispensable for large-scale multi-antenna systems, but is challenging to obtain. To tackle this issue, in this paper we propose a unified precoding and pilot design framework, that allows minimal and precoding-sensitive modified CSI (mCSI) to be collected. This results in a significant reduction in the CSI overheads and complexity compared to classical physical CSI (pCSI) estimation. Based on this unified framework, we further propose an intelligent pilot (IP) approach that senses and selects the mCSI to be collected. The IP approach utilizes a compressive sensing formulation to attach sensing and selection of significant mCSI to precoding optimization. We apply the above techniques to the multi-user frequency division duplexing (FDD) downlink as an example. Our study shows that the advantages of the IP approach are three-fold. First, in contrast to the pCSI, precoding-sensitive information is only captured, which reduces the training and feedback overheads. Second, the precoders are optimized directly based on the mCSI, which avoids recovering the pCSI of high-dimension. Third, since the mCSI of reduced dimension is utilized, the scale of the problem to optimize the precoder is also reduced and thus it is much easier to solve.**

***Index Terms*—Intelligent pilot design, intelligent modified CSI selection, precoding and pilot design, contextual bandit learning, symbol-level precoding, intelligent wireless communication.**

I. Introduction

Its high spectrum and energy efficiency and tolerance to simple signal processing techniques have established massive multiple-input multiple-output (MIMO) as a key 5G technology [1]. Massive MIMO employs a large number of antennas at base station (BS) to serve multiple users (UEs) simultaneously. To reap these benefits of massive MIMO, CSI between BS and UEs is often indispensable. However, due to the prohibitively high overhead associated with downlink training and uplink feedback, the acquisition of downlink CSI is recognized as a very challenging task for massive MIMO systems. This is particularly pronounced for the FDD massive MIMO systems, where the channel reciprocity between uplink channels and the downlink counterparts cannot be exploited [2].

To overcome these challenges and acquire CSI of massive MIMO systems with reduced overheads, a variety of methods have been proposed in the past several years, which roughly fall into three categories. For the first category, frequency-independent non-statistical information (e.g., sparsity of high-frequency channels or angular and delay reciprocities between uplink and downlink channels) are exploited to acquire CSI, so as to reduce the training overhead [3]–[5]. For the second category, channel statistics (e.g., channel correlation or channel covariance matrix) are exploited to acquire CSI with lower overheads [6]–[10]. Recently, machine learning (in particular, deep learning) has inspired learning-based CSI acquisition methods, which constitute the third category [11]–[13].

As an effective means to improve the system performance, precoding has always been an active research area in wireless communications. Given that perfect CSI is available, various precoding algorithms have been proposed [14]–[18]. Note that in classical approaches, interferences are often regarded as a limitation and are suppressed as much as possible. However, seen from an instantaneous point of view, interferences can be constructive and can also be exploited through symbol-level precoding (SLP). The concept of constructive interference (CI) was exploited to improve the system performance in [19]–[23]. In particular, a low-complexity vector precoding scheme was proposed in [23] for limited feedback downlink multi-user MISO systems, which is the first work on optimization based CI precoding. This was followed by [24] first proposing an explicit precoding optimization based on CI with strict angle constraints, and in [25] extended to a CSI-robust CI precoder with a relaxed optimization. The idea of CI exploitation has been extended to various scenarios/applications [26]–[32].

For most precoding algorithms, perfect pCSI is assumed, which is, however, challenging (and even impossible) to obtain in practice. To deal with this issue, robust precoding algorithms have been proposed in [25], [33]–[35]. Note that in relevant literatures, desired performance metric unidirectionally depends on CSI estimation (via precoder optimization). Typically, CSI acquisition and precoding optimization are often tackled separately. On the one hand, various algorithms have been proposed to estimate pCSI as accurately as possible, however, without considering the subsequent precoding design. On the other hand, precoders are optimized under the assumption that estimated or even perfect pCSI is available. However, the conventional unidirectional and separate design paradigm not only increases design complexity, but also may lead to some performance loss. Firstly, the overheads of training and feedback are prohibitively high, which makes it challenging to obtain complete pCSI. Secondly, the complete pCSI may not be a necessity (e.g., it may consist of superfluous information). Thirdly, because of the unidirectional dependency relationship, the desired or required pCSI, however, may not be estimated. Finally, it is challenging to realize a scalable tradeoff between a performance metric of interest (PMoI) and the training and/or feedback overheads.

The work was supported by the Engineering and Physical Sciences Research Council, U.K. under project EP/S028455/1. (Corresponding author: Jianjun Zhang.)

J. Zhang and C. Masouros are with the Department of Electronic & Electrical Engineering, University College London, London WC1E7JE, U.K. (E-mail: {jianjun.zhang,c.masouros}@ucl.ac.uk).

To simplify system design and improve the PMoI, algorithms that directly employ the mCSI to design precoders have been proposed in millimeter wave (mmwave) communications, by exploiting channel sparsity [36]–[38]. In particular, CSI acquisition (via beam training and tracking) and precoding optimization were jointly considered in [37] for multi-user mmwave communication systems. The joint design of CSI acquisition and precoding optimization in mmwave communication relies heavily on the fact that the power angular spectrum (PAS) of mmwave channels is discrete. It is problematic to directly extend these algorithms to FDD massive MIMO communications, because the PAS of FDD channels is often continuous and may have a large angle spread. The joint design becomes more challenging when it comes to multi-user FDD downlink communications, since the overhead of CSI acquisition increases as more served users are involved. For this reason, efficient algorithms have not been investigated for the FDD downlink multi-user systems. As for more general correlated channels, both theoretical feasibility and effective algorithms are still unavailable.

To tackle the aforementioned issues, we propose a unified precoding and pilot design optimization (UPPiDO) framework and further implement it via IP in this paper. Within the framework, PMoI determines and guides mCSI estimation, and only significant and desired mCSI can be identified, selected, estimated and fed back. To fulfill the framework, we propose two support techniques, i.e., mCSI based precoding and pilot design (mCSI-PPD) and significant mCSI intelligent sensing and selection (mCSI-ISS). Based on the framework, we propose IP-based algorithms to jointly acquire CSI and optimize precoders with CI exploitation for FDD downlink multi-user systems. The proposed IP-based algorithms make full use of spatial correlation to reduce overheads of training and feedback. The other advantages are as follows. Firstly, only precoding-sensitive mCSI is captured, and thus the training and feedback overheads can be greatly reduced. Secondly, there is no need to reconstruct the original pCSI to design precoders, which simplifies system operations. Thirdly, since the precoders are optimized directly based on the mCSI of much reduced dimension, the scale of the problem to optimize the precoders is much smaller than that of the original optimization problem with complete pCSI, which is much easier to solve. Instead of using the complete (but inaccurate) pCSI, the use of a small amount of inaccurate significant mCSI helps to achieve a robust performance. The main contributions are summarized as follows:

- We propose a unified precoding and pilot design optimization (UPPiDO) framework implemented via IP. An algorithm designed based on the framework only estimates required mCSI, and the selection and identification of the required mCSI are implemented via designing precoders to optimize the PMoI.
- To implement the framework, we propose the mCSI-PPD technique, which enables to optimize pilot and precoder with training- and feedback-efficient mCSI. Particularly, we prove theoretically that for a major class of special precoding schemes, where the channel vectors and precoding vectors take the form of inner product, precoding-sensitive mCSI can be used instead to design precoders, which provides the theoretical foundation for UPPiDO.
- To obtain more efficient mCSI, we propose the mCSI-ISS technique, where significant mCSI is sensed and selected intelligently, using a compressive sensing formulation. In particular, automatic model selection technique via the $L1$ regularization is proposed to induce sparsity and select significant mCSI. To adapt to complex environments, we employ contextual bandit learning to design a learning-based algorithm to choose the regularization parameter.
- We take the challenging FDD downlink multi-user system as an example and propose both heuristic and learning-based algorithms to construct efficient IPs. Based on the IPs, we further propose an efficient SLP algorithm which jointly acquires mCSI and optimizes precoders.
- Comprehensive simulation results are provided to demonstrate the effectiveness and superiorities of the proposed algorithms, including: a more robust performance under inaccurate mCSI, a lower computational complexity (depending on the length of the IP, rather than the number of antennas), and a scalable tradeoff between performance of interest and training/feedback overhead.

The remainder of this paper is organized as follows. System model of FDD downlink multi-user CI-based SLP problem is described in Section II. Taking the FDD downlink multi-user CI-based SLP as an example, the mCSI-PPD and mCSI-ISS techniques are elaborated in Section III and Section IV, respectively. The simulation results are provided in Section V, and conclusions are given in Section VI.

Notations: Bold uppercase $\mathbf{A}$ and bold lowercase $\mathbf{a}$ denote matrices and column vectors, respectively. Without particular specification, non-bold letters A, a denote scalars. Caligraphic letters $\mathcal{A}$ stand for sets. $\mathbb{E}(\cdot)$ and $(\cdot)^{\mathrm{H}}$ denote the mathematical expectation and Hermitian operators, respectively. $\mathbb{I}\{\cdot\}$ and $\mathrm{card}(\mathcal{A})$ represent the indicator function and the cardinality of $\mathcal{A}$, respectively. $(\cdot)^\star$ represents an optimal quantity, e.g., an optimal solution of an optimization problem. $\mathcal{CN}(\mathbf{m}, \mathbf{R})$ stands for a complex Gaussian random vector with mean $\mathbf{m}$ and covariance matrix $\mathbf{R}$.

II. System Model

Consider an FDD downlink multi-user communication system, which consists of one BS equipped with N transmit antennas and U single-antenna users (UEs), as illustrated in Fig. 1. The set of the U UEs is denoted by $\mathcal{U} = \{1, 2, \cdots, U\}$. The UEs are randomly distributed in U regions. Without loss of generality, uniform linear array (ULA) is considered in this paper. The developed algorithms are also applicable to other antenna array geometries (e.g., uniform planar array - UPA). In fact, it is sufficient to reconstruct a corresponding codebook (e.g., by uniformly sampling a rectangular beam space for UPA) when applying to another antenna array geometry.

Under the assumption of ULA, the channel vector between

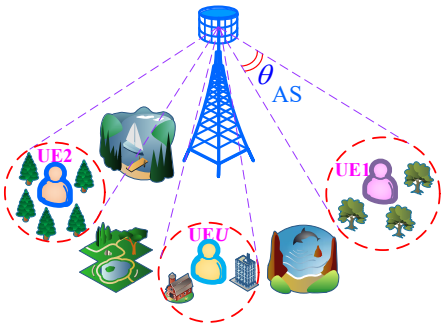

Fig. 1. Illustration of an FDD downlink multi-user communication system.

the BS and each UE $u \in \mathcal{U}$ can be expressed as [7], [11]

$$\begin{aligned}\bar{\mathbf{h}}_u &= \int_{\theta\in\mathcal{A}_u} g_u(\theta)\mathbf{a}(\theta)d\theta \\ &= \int_{\bar{\theta}_u-\Delta_u}^{\bar{\theta}_u+\Delta_u} |g_u(\theta)|e^{j\phi_u(\theta)}\mathbf{a}(\theta)d\theta, \end{aligned} \tag{1}$$

where $\mathcal{A}_u = [\bar{\theta}_u - \Delta_u, \bar{\theta}_u + \Delta_u]$ represents angle spread (AS) of UE u with Δ_u denoting single-side AS. $|g_u(\theta)|$ and $\phi_u(\theta)$ in (1) represent attenuation (amplitude) and random phase of signal ray from θ, respectively. $\mathbf{a}(\cdot)$ represents array response vector and takes the form

$$\mathbf{a}(x) = \frac{1}{\sqrt{N}}\left[1, e^{jx\frac{2\pi}{\lambda}d}, e^{jx\frac{2\pi}{\lambda}2d}, \cdots, e^{jx\frac{2\pi}{\lambda}(N-1)d}\right], \tag{2}$$

where λ and d denote the signal wave-length and the distance between any two adjacent antennas, respectively. Note that for more general or complex channel models, e.g., channel in (1) with multiple AS intervals or larger ASs, the developed algorithms can also be applied directly.

Without loss of generality, the PSK modulation (with constellation $\mathcal{S}_u$ of size K_u for UE u) is considered in this paper. Nevertheless the developed algorithms are also applicable to other modulations [39] [1]. Let $s_u = e^{j\xi_u} \in \mathcal{S}_u$ be the intended PSK information symbol for UE u (with ξ_u the argument of s_u) and $\mathbf{x}$ be the transmitted signal. Then, the signal received at each UE u can be written as

$$y_u = \bar{\mathbf{h}}_u^{\mathrm{H}}\mathbf{x} + n_u, \tag{3}$$

where $n_u \sim \mathcal{CN}(0, \sigma_{\mathrm{N}}^2)$ denotes random noise.

With the aim of improving energy efficiency, the idea of CI is exploited. For the PSK modulation, the key of the CI design principle can be captured by the following constraints ($\forall\, u \in \mathcal{U}$) [25]

$$\left|\mathrm{Im}(\bar{\mathbf{h}}_u^{\mathrm{H}}\mathbf{x}e^{-j\xi_u})\right| \le \left(\mathrm{Re}(\bar{\mathbf{h}}_u^{\mathrm{H}}\mathbf{x}e^{-j\xi_u}) - \gamma_u\right)\tan(\pi/K_u), \tag{4}$$

where γ_u is an SNR metric that measures the quality of received signal of UE u. The above design constraints enforce that the CI pushes the received signal away from the decision boundaries of the PSK constellation. The reader is referred to [40] for more details. Next, we adopt the power-minimization SLP as an example, which can be formulated as [25]

$$\begin{aligned}\min_{\mathbf{x}}\quad & \|\mathbf{x}\|^2 \\ \text{s.t.}\quad & \left|\mathrm{Im}(\bar{\mathbf{h}}_u^{\mathrm{H}}\mathbf{x}e^{-j\xi_u})\right| \le \\ & \left(\mathrm{Re}(\bar{\mathbf{h}}_u^{\mathrm{H}}\mathbf{x}e^{-j\xi_u}) - \gamma_u\right)\tan(\pi/K_u),\ (\forall\, u \in \mathcal{U}).\end{aligned} \tag{5}$$

It is not difficult to solve problem (5), if the pCSI, i.e., $\{\bar{\mathbf{h}}_u\}$, is available. In fact, problem (5) is a second-order cone programming [23], which can be efficiently solved via convex optimization tools, such as CVX or CVXOPT. However, it is difficult to obtain highly-precise CSI in practice. In particular, in contrast to TDD, where the downlink CSI can be obtained from the uplink counterpart by using the channel reciprocity, the downlink CSI is conventionally obtained via downlink training and uplink feedback for an FDD system. However, the overheads of both downlink training and uplink feedback are prohibitively high for a large-scale antenna array system. Furthermore, the CSI feedback is subject to quantization and noise errors. Next, we will address this issue via IP.

III. Modified CSI based Pilot and Precoding Design

The implementation of the UPPiDO framework incorporates two key support techniques, i.e., mCSI-PPD and mCSI-ISS. The individual roles of the two techniques are as follows:

- mCSI-PPD: The key to reduce the overheads of training and feedback is to exploit channel sparsity. However, pCSI is often not sparse. To obtain sparsity, mCSI-PPD jointly optimizes pilot and precoder in another domain, where the corresponding mCSI is sparse. The sparsity of mCSI enables efficient training and feedback, and helps to achieve a robust performance.
- mCSI-ISS: Even though the mCSI is sparse, it may still contain redundant and/or inaccurate information. To this end, we propose to identify and select significant mCSI. However, a heuristic method inevitably incurs a performance loss. To address this issue, automatic model selection via the $L1$ regularization is utilized to induce, identify and select significant mCSI.

In this section, we elaborate on the mCSI-PPD technique. Specifically, we first provide mathematical foundation for mCSI-PPD. Then, we propose two efficient heuristic methods to construct IPs for the FDD downlink multi-user system.

A. Mathematical Foundation of mCSI-PPD

Let $\bar{\mathbf{h}}_u$ and $\mathbf{v}_u \in \mathbb{C}^n$ denote physical channel vector and precoding vector of UE u, respectively. For convenience, let $\{\bar{\mathbf{h}}_u^{\mathrm{H}}\mathbf{v}_w\}$ collect all terms that take the form of inner product between the channel vectors and precoding vectors, i.e.,

$$\{\bar{\mathbf{h}}_u^{\mathrm{H}}\mathbf{v}_w\} = \{\bar{\mathbf{h}}_u^{\mathrm{H}}\mathbf{v}_w \,|\, u \in \mathcal{U}, w \in \mathcal{U}\}. \tag{6}$$

In general, the problem of precoding design can be formulated as

$$\begin{aligned}\min_{\{\mathbf{v}_w\}}\quad & f\big(\{\bar{\mathbf{h}}_u^{\mathrm{H}}\mathbf{v}_w\}\big) \\ \text{s.t.}\quad & h_i\big(\{\bar{\mathbf{h}}_u^{\mathrm{H}}\mathbf{v}_w\}\big) = 0,\ (i = 1, \cdots, I) \\ & g_j\big(\{\bar{\mathbf{h}}_u^{\mathrm{H}}\mathbf{v}_w\}\big) \le 0,\ (j = 1, \cdots, J),\end{aligned} \tag{7}$$

[1]For an arbitrary modulation mode (e.g., QAM and APSK), the problem of precoding design can almost always be formulated as an optimization problem, which is often a special case of the general problem in (7). The algorithms in this paper (e.g., Algorithm 3 or 4) are developed to address the general problem in (7), which can also be applied to address a special case.

where $h_i(\cdot) = 0\,(i = 1, \cdots, I)$ are equality constraints, and $g_j(\cdot) \leq 0\,(j = 1, \cdots, J)$ are inequality constraints.

It should be highlighted that in problem (7), none of the physical channel vectors $\{\bar{\mathbf{h}}_u\}$ emerges alone. They always take the form of inner product with the precoding vectors. It seems that this requirement is restrictive. However, the form in problem (7) is very general and contains many precoding designs of interest, e.g., the linear precoding. In fact, the only requirement is that $\{\bar{\mathbf{h}}_u\}$ and optimization variables of interest satisfy the form of inner product, e.g., problem (5) is an example. [2]. Another example is the classical problem of maximizing the system sum-rate, i.e.,

$$\begin{aligned} \max_{\{\mathbf{v}_u\}} \ & \sum_{u\in\mathcal{U}} \log\left(1 + \frac{\left|\bar{\mathbf{h}}_u^{\mathrm{H}}\mathbf{v}_u\right|^2}{\sum_{w\neq u}\left|\bar{\mathbf{h}}_u^{\mathrm{H}}\mathbf{v}_w\right|^2 + \sigma^2}\right) \\ \text{s.t.} \ & \sum_{u\in\mathcal{U}} \|\mathbf{v}_u\|^2 \leq P_{\mathrm{m}}, \end{aligned} \tag{8}$$

where σ^2 and P_{m} represent noise power and transmit power budget, respectively.

The following theorem provides theoretical foundation for mCSI-PPD, i.e., to optimize pilot and precoder via mCSI.

Theorem 1. *Let* $\mathbf{F}$ *be a matrix such that the set of all column vectors of* $\mathbf{F}$*, denoted by* $\mathcal{F}$*, spans vector space* $\mathbb{C}^N$*. Then, the problem in* (7) *is equivalent to the following problem*

$$\begin{aligned} \min_{\{\mathbf{y}_w\}} \quad & f\big(\{\bar{\mathbf{h}}_u^H\mathbf{F}\mathbf{y}_w\}\big) \\ s.t. \quad & h_i\big(\{\bar{\mathbf{h}}_u^H\mathbf{F}\mathbf{y}_w\}\big) = 0,\ (i = 1, \cdots, I) \\ & g_j\big(\{\bar{\mathbf{h}}_u^H\mathbf{F}\mathbf{y}_w\}\big) \leq 0,\ (j = 1, \cdots, J). \end{aligned} \tag{9}$$

Specifically, let set $\{\mathbf{y}_w^\star\}$ *be an optimal solution of problem* (9)*. Then, the set* $\{\mathbf{v}_w^\star = \mathbf{F}\mathbf{y}_w^\star\}$ *is an optimal solution of problem* (7)*.*

Proof: See Appendix A. ∎

Theorem 1 indicates that to solve problem (7), it is sufficient to solve the equivalent optimization problem in (9). Compared to the original problem in (7), the advantage of the equivalent problem in (9) is that there is no need to estimate the original pCSI $\{\bar{\mathbf{h}}_u\}$. Instead, if the mCSI, defined as $\{\mathbf{h}_u = \mathbf{F}^{\mathrm{H}}\bar{\mathbf{h}}_u\}$, is available, an efficient precoder can still be obtained. More importantly, by designing $\mathbf{F}$ (or $\mathcal{F}$) elaborately, the acquisition of $\{\mathbf{F}^{\mathrm{H}}\bar{\mathbf{h}}_u\}$ may be much easier, e.g., less training overhead. For example, via appropriate design, $\{\mathbf{F}^{\mathrm{H}}\bar{\mathbf{h}}_u\}$ may be sparse, and thus CSI acquisition becomes feedback-efficient.

Remark 3.1 Although precoding optimization in the beam domain was considered in [36], [37], theoretical feasibility and optimality were not provided. Theorem 1 not only theoretically confirms the feasibility and optimality, but also greatly extends original special cases (e.g., using DFT codebooks) to considerably general cases. In particular, Theorem 1 points out that only the very week condition is required to optimize pilot and precoder via mCSI, without loss of optimality. Theorem 1 lays the foundation of the UPPiDO framework.

Since $\mathcal{F}$ plays the role of estimating the mCSI, it can be reasonably referred to as pilot. However, $\mathcal{F}$ itself often provides redundant or needless information and thus is inefficient. To alleviate the difficulty of acquiring and feeding back the mCSI, all that is needed is a small subset $\mathcal{F}_0 \subset \mathcal{F}$ chosen carefully from $\mathcal{F}$ which can capture sufficient channel information and enable to design an efficient precoder. If such a subset $\mathcal{F}_0$ exists, it is referred to as an IP, which is defined as follows.

Definition 1 (Intelligent Pilot)**.** *A subset of* $\mathcal{F}$ *is referred to as an IP if it has the following properties or features:*

- *The IP can sense and capture precoding-sensitive information (PSI) with low training overhead. Moreover, the PSI can also be fed back from UEs to the BS efficiently.*
- *With the PSI available, the BS can design efficient precoders of interest directly. In particular, there is no need to reconstruct complete physical channels.*

The set $\mathcal{F}$ in Definition 1 is referred to as pre-pilot or pre-IP. Note that the IP in Definition 1 is defined from the perspective of efficiently sensing and capturing PSI to design precoders. In the next section, we will pay more attentions to design IPs which can adapt to channel environments.

B. IP Design for FDD Downlink Multi-User System

As an application of Theorem 1, we propose two heuristic methods to construct IPs for the FDD downlink multi-user system. The first step is to choose an appropriate pre-pilot $\mathcal{F}$ (or $\mathbf{F}$). In view of the channel model in (1), the widely used DFT codebook is chosen as the pre-pilot $\mathcal{F}$, which is constructed by uniformly sampling the entire beam space $[-1, 1]$, i.e.,

$$\mathcal{C}_{\text{DFT}} = \{\mathbf{a}_i \,|\, \mathbf{a}_i = \mathbf{a}(-1 + 2i/N), i = 0, \cdots, N-1\}.$$

Another typical choice is dense codebook (DC), obtained by sampling the beam space more densely. [3] If the size of a DC is L times as large as that of the standard DFT codebook (of size N), the DC is referred to as L-DC and denoted by $\mathcal{C}_{L\text{-DC}}$, i.e.,

$$\mathcal{C}_{L\text{-DC}} = \big\{\mathbf{a}_i \,\big|\, \mathbf{a}_i = \mathbf{a}\big(-1 + 2i/(LN)\big), i = 0, \cdots, LN-1\big\}.$$

Next, we construct an IP for each UE, and without loss of generality, we focus on UE u. To construct an IP, we shall first analyze the channel covariance matrix. The downlink channel covariance matrix of UE u can be written as

$$\begin{aligned} \mathbf{R}_u &= \int_{\theta\in\mathcal{A}_u} \mathbb{E}\big[|g_u(\theta)|^2\big]\mathbf{a}(\theta)\mathbf{a}^{\mathrm{H}}(\theta)d\theta \\ &= \int_{\bar{\theta}_u-\Delta_u}^{\bar{\theta}_u+\Delta_u} S_u(\theta)\mathbf{a}(\theta)\mathbf{a}^{\mathrm{H}}(\theta)d\theta, \end{aligned} \tag{10}$$

where $S_u(\theta) = \mathbb{E}[|g_u(\theta)|^2]$ is the PAS function of channel $\bar{\mathbf{h}}_u$ and characterizes the channel power distribution in the angular domain [7], [41]. Note that $S_u(\theta)$ is continuous and compactly

[2]The precoded transmit vector $\mathbf{x}$ in a MU-MISO system takes the form $\mathbf{x} = [\mathbf{v}_1, \mathbf{v}_2, \cdots, \mathbf{v}_K]\mathbf{s} = \mathbf{V}\mathbf{s}$, where $\mathbf{s}$ is transmitted data vector. From the view of system implementation, we are more concerned about $\mathbf{x}$. In classical precoding, each precoding vector $\mathbf{v}_k$ is optimized explicitly and shared by all data vectors, based on which $\mathbf{x}$ can be obtained easily. In SLP, each component of $\mathbf{s}$ is chosen from a constellation of finite size, which enables us to directly optimize $\mathbf{x}$, instead of $\mathbf{V}$.

[3]To obtain more efficient IPs, the pre-pilot $\mathcal{F}$ should be optimized as well. Due to space limitation, this is deferred to our future work.

supported in $\mathcal{A}_u = [\bar{\theta}_u - \Delta_u, \bar{\theta}_u + \Delta_u]$, i.e., $\mathcal{A}_u$ is the support (i.e., non-zero region) of the function $S_u(\theta)$.

Let $\mathcal{F}_u$ be the set of beams such that the main-lobe of each element of $\mathcal{F}_u$ is within the support of $S_u(\theta)$, i.e.,

$$\mathcal{F}_u = \{\mathbf{a}(\theta) \in \mathcal{F} \,|\, S_u(\theta) \geq \varepsilon > 0\}, \tag{11}$$

where the pre-pilot is chosen as $\mathcal{C}_{\text{DFT}}$ or $\mathcal{C}_{L\text{-DC}}$ (i.e., $\mathcal{F} = \mathcal{C}_{\text{DFT}}$ or $\mathcal{F} = \mathcal{C}_{L\text{-DC}}$) and ε is a small real number. Then, an efficient IP can be constructed as

$$\mathcal{P}_\theta = \bigcup_{u=1}^{U} \mathcal{F}_u. \tag{12}$$

The IP in (12) constructed based on the PAS functions $\{S_u(\theta)\}$ is denoted by $\mathcal{P}_\theta$. Accordingly, the matrix that collects all vectors in $\mathcal{P}_\theta$ is denoted by $\mathbf{P}_\theta$.

Each element or codeword in $\mathcal{P}_\theta$ is referred to as a pilot beam. Given $\mathbf{P}_\theta$, the physical channel vector $\bar{\mathbf{h}}_u$ can be mapped into the beam (or angular) domain, i.e.,

$$\mathbf{h}_u = \mathbf{P}_\theta^{\text{H}} \bar{\mathbf{h}}_u. \tag{13}$$

It is observed that compared to the original physical channel vector $\bar{\mathbf{h}}_u$, the dimension of $\mathbf{h}_u$ has been reduced, and thus $\mathbf{h}_u$ is feedback-efficient. Similarly, to estimate $\mathbf{h}_u$, it is sufficient to transmit all pilot beams in $\mathcal{P}_\theta$, which implies that $\mathcal{P}_\theta$ is training-efficient. Note also that $\{\mathbf{h}_u\}$ can be used to design efficient precoders, as shown in the next subsection. According to Definition 1, $\mathcal{P}_\theta$ can be referred to as an IP. Accordingly, $\{\mathbf{h}_u\}$ are the PSI corresponding to $\mathcal{P}_\theta$.

In some cases, the IP $\mathcal{P}_\theta$ may be very large, which may lead to a prohibitively large overhead in terms of both training and feedback. Next, we further propose a superposed multiple beam (SMB) technique to alleviate this issue. Via appropriate user scheduling, it is not difficult to guarantee that the supports of PASs of U UEs are non-overlapping, i.e.,

$$\mathcal{A}_u \cap \mathcal{A}_v \approx \emptyset, \ (\forall\, u \neq v, u \in \mathcal{U}, v \in \mathcal{U}).$$

In this case, the array response vectors constructed from the supports of any two UEs are approximately orthogonal, i.e.,

$$|\mathbf{a}^{\text{H}}(\theta_u)\mathbf{a}(\theta_v)| \approx 0, \ (\forall\, \theta_u \in \mathcal{A}_u, \theta_v \in \mathcal{A}_v, u \neq v). \tag{14}$$

For convenience, each set $\mathcal{F}_u$ can be explicitly written as

$$\mathcal{F}_u = \{\mathbf{a}(\theta_{u,1}), \mathbf{a}(\theta_{u,2}), \cdots, \mathbf{a}(\theta_{u,I_u})\}, \tag{15}$$

where $I_u = |\mathcal{F}_u|$ represents the size of $\mathcal{F}_u$.

Let $\mathbf{\Theta}$ collect all angle values, i.e., $\mathbf{\Theta} = \{\theta_{u,i} \,|\, 1 \leq u \leq U, 1 \leq i \leq I_u\}$. The SMB technique essentially divides set Θ into several subsets $\mathcal{D}_1, \cdots, \mathcal{D}_K$ such that $\Theta = \mathcal{D}_1 \cup \cdots \cup \mathcal{D}_K$ holds (but $\mathcal{D}_i \cap \mathcal{D}_j \neq \emptyset$ may hold). Then, another IP, denoted by $\mathcal{P}'_\theta$, can be defined as

$$\mathcal{P}'_\theta = \left\{ \mathbf{p}_k = \sum_{\theta \in \mathcal{D}_k} \mathbf{a}(\theta) \right\}. \tag{16}$$

For each subset $\mathcal{D}_k$, the superposed beam is constructed as

$$\mathbf{p}_k = \sum_{\theta \in \mathcal{D}_k} \mathbf{a}(\theta). \tag{17}$$

To reduce interferences among multiple beams within each superposed beam $\mathbf{p}_k$, the SMB technique makes full use of a basic property of general antenna arrays, i.e., if the distance [4], denoted by $\delta(\cdot,\cdot)$, between two angle values is large, the mutual interference between the two corresponding beams is small. Based on this property, we propose two principles to divide $\mathbf{\Theta}$ to further construct IPs: (1) $\text{card}(\mathcal{F}_u \cap \mathcal{D}_k) \leq 1\,(\forall\, u \,\text{and}\, k)$, i.e., each superposed beam consists of at most one beam from an arbitrary user; (2) Let $d(\mathcal{D}_k) = \min_{\theta_i \neq \theta_j, \theta_i \in \mathcal{D}_k, \theta_j \in \mathcal{D}_k} \delta(\theta_i, \theta_j)$, i.e., the minimum distance between any two different elements in $\mathcal{D}_k$. Then, $\min\{d(\mathcal{D}_1), \cdots, d(\mathcal{D}_K)\}$ should be maximized, so as to reduce the interferences.

Based on the above two principles, we can construct an efficient IP for a general antenna array geometry or channel model. In particular, with the assumption that $I_1 = I_2 = \cdots = I_U$ holds and the angle values $\{\theta_{u,i}\}$ satisfy the following inequalities

$$\begin{aligned} &\theta_{1,1} < \theta_{1,2} < \cdots < \theta_{1,I_1} < \\ &\theta_{2,1} < \theta_{2,2} < \cdots < \theta_{2,I_2} < \\ &\quad \cdots \\ &\theta_{U,1} < \theta_{U,2} < \cdots < \theta_{U,I_U}, \end{aligned} \tag{18}$$

the IP can be explicitly constructed as

$$\mathcal{P}'_\theta = \left\{ \mathbf{p}_i = \sum_{u=1}^{U} \mathbf{a}(\theta_{u,i}) \,\middle|\, i = 1, \cdots, I_U \right\}. \tag{19}$$

Similarly, the matrix collecting all vectors in $\mathcal{P}'_\theta$ is denoted by $\mathbf{P}'_\theta$. Note that compared to $\mathcal{P}_\theta$, each element in $\mathcal{P}'_\theta$ (e.g., $\mathbf{p}_i \in \mathcal{P}'_\theta$), in fact, corresponds to multiple beams (or peaks), as shown in Fig. 2. Moreover, the overhead of training or feedback of $\mathcal{P}'_\theta$ has become $1/U$ of that of $\mathcal{P}_\theta$.

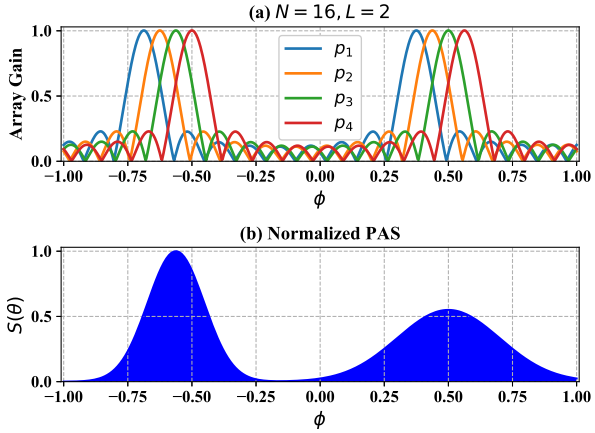

Fig. 2. An illustration of IP design via superposed multiple beam sensing.

Based on the above discussion, we can present an efficient algorithm to construct IPs for the FDD downlink multi-user system, which is summarized in Algorithm 1 for clarity. The

[4]The distance should characterize or measure the interference between two beams, which often depends on the antenna array geometry. We take the ULA as an example. The distance between two angle values x_1 and x_2 can be defined as $d(x_1, x_2) = \min_{m,n} |x_1 \bmod 2m\pi - x_2 \bmod 2n\pi|$.

Algorithm 1: IP for FDD Downlink Multi-user System

1: **input:** codebook $\mathcal{C}$ and support of PAS of each UE
2: **construct** training beam set $\mathcal{F}_u$ for each UE u according to its PAS support $\mathcal{A}_u$
3: **construct** IP $\mathcal{P}_\theta$ according to (12) or ($\mathcal{P}'_\theta$ using the SMB technique according to (19))
4: **transmit** signals with each pilot beam $\mathbf{p}_i \in \mathcal{P}_\theta$ (or $\mathbf{p}_i \in \mathcal{P}'_\theta$)
5: **process** received signals and feed them back to BS
6: **design** a precoder and perform data transmission

BS first estimates the PAS support of each UE and ensures that the supports of the served UEs are non-overlapped. In step 2, the BS constructs beam training set $\mathcal{F}_u$ according to (11). An IP can be constructed according to (12) (or (19) by using the SMB technique) in step 3. Then the BS transmits signals based on the constructed IP (in step 4). Via appropriate processing, the UEs feed back the PSI to the BS. Although there may exist other more efficient methods to obtain PSI (i.e., to design neural networks), in this paper we only consider the simplest method (i.e., the UEs simply quantize the received signals and then feed them back to the BS), so as to simplify the operations of UEs. Finally, the BS regards the received signals as the PSI and uses them to design a precoder to transmit effective data. More details will be provided in the next subsection.

The PAS supports required by Algorithm 1 can be estimated by using the algorithm in [7]. However, the heuristic construction of $\mathcal{P}_\theta$ and $\mathcal{P}'_\theta$ inevitably leads to a performance loss. To alleviate the requirement of estimating the PAS supports and further improve the system performance, we will propose the mCSI-ISS technique to intelligently sense, identify and select significant mCSI. But, before that, we shall first propose an efficient SLP algorithm to show how to exploit the PSI.

C. Symbol-Level Precoding via IP

To design a precoder, we require the following corollary, which can be directly obtained from Theorem 1.

Corollary 1. *The problem in* (5) *is equivalent to the following optimization problem*

$$\begin{aligned} \min_{\mathbf{d}} \quad & \|\mathbf{F}\mathbf{d}\|^2 \\ \textit{s.t.} \quad & \left|\mathrm{Im}(\bar{\mathbf{h}}_u^{\mathrm{H}}\mathbf{F}\mathbf{d}e^{-j\xi_u})\right| \le \\ & \left(\mathrm{Re}(\bar{\mathbf{h}}_u^{\mathrm{H}}\mathbf{F}\mathbf{d}e^{-j\xi_u}) - \gamma_u\right)\tan(\pi/K_u),\ (\forall\, u \in \mathcal{U}). \end{aligned} \tag{20}$$

Corollary 1 indicates that to design an efficient precoder via solving problem (5), it is sufficient to solve the equivalent problem in (20), for which we only need to estimate the mCSI $\{\mathbf{h}_u = \mathbf{F}^{\mathrm{H}}\bar{\mathbf{h}}_u\}$. Note that $\{\mathbf{h}_u\}$ can be estimated via IPs. We take $\mathcal{P}'_\theta$ as an example, and it is similar for $\mathcal{P}_\theta$.

Let $\mathbf{P}'_\theta = [\mathbf{p}_1, \cdots, \mathbf{p}_{I_U}]$ with each $\mathbf{p}_i \in \mathcal{P}'_\theta$. Instead of estimating $\{\bar{\mathbf{h}}_u\}$, an estimation of $\{\mathbf{P}'^{\mathrm{H}}_\theta\bar{\mathbf{h}}_u\}$ can be obtained. A simple method is as follows. The BS sends training signal $s = 1$ along each pilot beam defined in $\mathcal{P}'_\theta$. For each $\mathbf{p}_i \in \mathcal{P}'_\theta$, the signal received by UE u can be written as

$$y_{u,i} = \bar{\mathbf{h}}_u^{\mathrm{H}}\mathbf{p}_i s + n_{u,i} = \bar{\mathbf{h}}_u^{\mathrm{H}}\mathbf{p}_i + n_{u,i}, \tag{21}$$

where $n_{u,i}$ is the noise variable. Then, each UE u quantizes the received signals $\{y_{u,i} \,|\, i = 1, \cdots, I_U\}$, which yields quantized signals $\{\hat{y}_{u,i} \,|\, i = 1, \cdots, I_U\}$. The quantized signals (i.e., PSI) are fed back to the BS by each UE.

Let $\Theta = \{\theta_j \,|\, \mathbf{a}(\theta_j) \in \mathcal{F}\}$. Then, with the PSI $\{\hat{y}_{u,i} \,|\, i = 1, \cdots, I_U\}$ available, $\{\mathbf{h}_u\}$ can be estimated as follows

$$\mathbf{h}_u(j) \approx \begin{cases} \bar{\mathbf{h}}_u^{\mathrm{H}}\mathbf{a}(\theta_{u,i}) \approx \bar{\mathbf{h}}_u^{\mathrm{H}}\mathbf{p}_i \approx \hat{y}_{u,i} & \theta_j = \theta_{u,i} \\ 0 & \text{otherwise,} \end{cases} \tag{22}$$

where $\mathbf{h}_u(j)$ denotes the j-th component/element of the vector $\mathbf{h}_u$. Let $\hat{\mathbf{h}}_u$ represent the estimation of $\mathbf{h}_u$. The SLP problem in (20) can be rewritten as

$$\begin{aligned} \max_{\mathbf{d}} \quad & \|\mathbf{F}\mathbf{d}\|^2 \\ \text{s.t.} \quad & \left|\mathrm{Im}(\hat{\mathbf{h}}_u^{\mathrm{H}}\mathbf{d}e^{-j\xi_u})\right| \le \\ & \left(\mathrm{Re}(\hat{\mathbf{h}}_u^{\mathrm{H}}\mathbf{d}e^{-j\xi_u}) - \gamma_u\right)\tan(\pi/K_u),\ (\forall\, u \in \mathcal{U}). \end{aligned} \tag{23}$$

Let matrix $\mathbf{A}$ collect all beams in all sets $\{\mathcal{F}_u\}$ of all UEs. Similarly, $\mathbf{h}'_u = \mathbf{A}^{\mathrm{H}}\bar{\mathbf{h}}_u$ can also be estimated based on $\{\hat{y}_{u,i}\}$. For convenience, $\mathbf{h}'_u$ is still denoted by $\mathbf{h}_u$. Then, the SLP problem in (5) or (23) can be equivalently written as

$$\begin{aligned} \max_{\mathbf{d}} \quad & \|\mathbf{A}\mathbf{d}\|^2 \\ \text{s.t.} \quad & \left|\mathrm{Im}(\hat{\mathbf{h}}_u^{\mathrm{H}}\mathbf{d}e^{-j\xi_u})\right| \le \\ & \left(\mathrm{Re}(\hat{\mathbf{h}}_u^{\mathrm{H}}\mathbf{d}e^{-j\xi_u}) - \gamma_u\right)\tan(\pi/K_u),\ (\forall\, u \in \mathcal{U}). \end{aligned} \tag{24}$$

Note that the dimension of the optimization variable in problem (24) (i.e., the scale of the optimization problem) is much lower than that of problem (5), and thus the computational complexity to solve problem (24) has been greatly reduced. This is another important advantage of the IP approach.

Algorithm 2: Symbol-Level Precoding Design via IP

1: **input:** PAS supports of U UEs
2: **construct** an IP to estimate PSI (via Algorithm 1)
3: **construct** optimization problem (23) or (24)
4: **solve** the constructed problem to obtain a precoder
5: **perform** data transmission by the precoder

Note that both problem (23) and problem (24) are convex and can be efficiently solved via interior-point methods. For clarity, the SLP algorithm is summarized in Algorithm 2. We first construct an IP according to Algorithm 1 and use the IP to obtain required PSI (in step 2). In step 3, we construct an optimization problem based on the estimated PSI. By solving the constructed optimization problem (in step 4), we can obtain a precoder and use it to transmit data (in step 5).

IV. Learning-based Unified Precoding and Intelligent Pilot Design

In the previous section, the mCSI is identified and selected heuristically. Moreover, only information of PAS supports of UEs has been utilized, while other useful information (e.g., shape of the PAS function) has been discarded. In this section,

we propose the mCSI-ISS technique to intelligently sense and select significant mCSI, which has three appealing advantages. Firstly, the most significant mCSI is automatically identified and selected, without explicitly estimating the PAS function (and the PAS support). Secondly, the mCSI-ISS technique can make full use of the PAS information, including the shape of the PAS function. Finally, the IP approach incorporating the mCSI-ISS technique can adapt to channel environments.

A. Intelligent Sensing and Selection of Significant mCSI

To reap the aforementioned benefits, we need to reformulate problem (20) (in Corollary 1) as follows

$$\begin{aligned} \min_{\mathbf{d}} \quad & \|\mathbf{F}\mathbf{d}\|_2^2 + \rho\|\mathbf{d}\|_1 \\ \text{s.t.} \quad & \left|\mathrm{Im}(\bar{\mathbf{h}}_u^{\mathrm{H}}\mathbf{F}\mathbf{d}e^{-j\xi_u})\right| \leq \\ & \quad \Big(\mathrm{Re}(\bar{\mathbf{h}}_u^{\mathrm{H}}\mathbf{F}\mathbf{d}e^{-j\xi_u}) - \gamma_u\Big)\tan(\pi/K_u),\ (\forall\, u \in \mathcal{U}). \end{aligned} \tag{25}$$

where $\rho > 0$ denotes regularization parameter. Compared to the previous optimization problems, e.g., problem (23), an $L1$ regularization term $\rho\|\mathbf{d}\|_1$ is introduced. Because of the $L1$ regularization term $\rho\|\mathbf{d}\|_1$, solving problem (25) will induce a sparse solution, based on which the significant mCSI can be identified/determined. This technique is referred to as mCSI-ISS.

Remark 4.1 It is crucial to introduce the $L1$ regularization term. On the one hand, from the perspective of machine learning, the regularization term plays the role of automatic model selection. Hence, the most significant mCSI required to design precoders can be automatically identified and selected by solving problem (25). On the other hand, from the perspective of optimization theory, the regularization term (which should be referred to as penalty term in this case) facilitates to generate a sparse solution automatically. Accordingly, the training and feedback overheads can be reduced. This automation process avoids explicitly accessing to the PAS function (or its support) and possible performance loss (due to an inaccurate estimation or inappropriate use of the PAS).

Remark 4.2 In fact, the IP design is often a combinational optimization problem, which is difficult to tackle. In general, only heuristic solutions can be obtained. However, via the reformulation in (25), it is cast into a continuous optimization problem, which can be solved efficiently. A large number of simulation experiments show that the mCSI-ISS technique offers very good performance and indeed significantly outperforms the state of the art, e.g., in terms of training and feedback overheads.

Remark 4.3 It is important to distinguish between compressive sensing (CS) based channel estimations and the mCSI-ISS technique. The objective of the CS-based methods is to recover the complete pCSI by using as few measurements as possible. However, the goal of the mCSI-ISS technique is to capture PSI to design precoders at a minimum cost.

Before proceeding, we show how to extend the formulation in (25) to the general problem of precoding design in (9). In fact, by using the mCSI-ISS technique, problem (9) can be reformulated as

$$\begin{aligned} \min_{\{\mathbf{y}_w\}} \quad & f\big(\{\bar{\mathbf{h}}_u^{\mathrm{H}}\mathbf{F}\mathbf{y}_w\}\big) + \rho\sum_w \|\mathbf{y}_w\|_1 \\ \text{s.t.} \quad & h_i\big(\{\bar{\mathbf{h}}_u^{\mathrm{H}}\mathbf{F}\mathbf{y}_w\}\big) = 0,\ (i = 1, \cdots, I) \\ & g_j\big(\{\bar{\mathbf{h}}_u^{\mathrm{H}}\mathbf{F}\mathbf{y}_w\}\big) \leq 0,\ (j = 1, \cdots, J). \end{aligned} \tag{26}$$

As an example, the classical sum-rate maximization problem in (8) can be expressed as

$$\begin{aligned} \max_{\{\mathbf{y}_u\}} \quad & \sum_{u\in\mathcal{U}} \log\left(1 + \frac{\left|\bar{\mathbf{h}}_u^{\mathrm{H}}\mathbf{F}\mathbf{y}_u\right|^2}{\sum_{w\neq u}\left|\bar{\mathbf{h}}_u^{\mathrm{H}}\mathbf{F}\mathbf{y}_w\right|^2 + \sigma^2}\right) \\ & \quad - \rho\sum_u \|\mathbf{y}_u\|_1 \\ \text{s.t.} \quad & \sum_{u\in\mathcal{U}} \|\mathbf{F}\mathbf{y}_u\|^2 \leq P_{\mathrm{m}}. \end{aligned} \tag{27}$$

Note that with the formulation in (26) available, Algorithms 3 and 4 can be employed directly.

Temporarily, we assume that an optimal value of the regularization parameter, denoted by $\rho^\star$, has been obtained. Later, we will propose a learning-based algorithm to find the optimal value. With $\rho^\star$ available, we can design an efficient algorithm to determine an IP automatically. First, we use all beams in $\mathcal{F}$ to sweep the beam (or angular) space [5], and we can obtain an estimation of each $\mathbf{h}_u = \mathbf{F}^{\mathrm{H}}\bar{\mathbf{h}}_u$, which is denoted by $\hat{\mathbf{h}}_u$. Then, we construct the following optimization problem

$$\begin{aligned} \min_{\mathbf{d}} \quad & \|\mathbf{F}\mathbf{d}\|_2^2 + \rho^\star\|\mathbf{d}\|_1 \\ \text{s.t.} \quad & \left|\mathrm{Im}(\hat{\mathbf{h}}_u^{\mathrm{H}}\mathbf{d}e^{-j\xi_u})\right| \leq \\ & \quad \Big(\mathrm{Re}(\hat{\mathbf{h}}_u^{\mathrm{H}}\mathbf{d}e^{-j\xi_u}) - \gamma_u\Big)\tan(\pi/K_u),\ (\forall\, u \in \mathcal{U}). \end{aligned} \tag{28}$$

By solving problem (28), we can obtain an optimal solution $\mathbf{d}^\star$, which is sparse. Let the index set of non-zero components (or the components whose absolute values are greater than a small threshold value $\varepsilon > 0$) of vector $\mathbf{d}^\star$ be $\mathcal{I}(\mathbf{d}^\star)$, i.e.,

$$\mathcal{I}(\mathbf{d}^\star) = \{i \,|\, 0 < |\mathbf{d}(i)|\} \quad (\text{or } \mathcal{I}(\mathbf{d}^\star) = \{i \,|\, \varepsilon < |\mathbf{d}(i)|\}).$$

To improve reliability, in practice the above operations can be repeated K times, and the final index set is the union of the K index sets. Then, the components of each $\hat{\mathbf{h}}_u$ whose indices are within $\mathcal{I}(\mathbf{d}^\star)$ are the required PSI, and the beams used to estimate the PSI constitute an IP. For clarity, the approach to design an IP is summarized in Algorithm 3.

Algorithm 3: IP via Automatic Pilot Beam Selection
1: **input:** regularization parameter ρ
2: **sweep** beam space with $\mathcal{F}$ to estimate $\{\hat{\mathbf{h}}_u\}$
3: **construct** optimization problem (28) with $\{\hat{\mathbf{h}}_u\}$
4: **solve** optimization problem (28) $\Longrightarrow$ index set $\mathcal{I}_1$
5: **repeat** operations of step 2 to step 4 K times $\Longrightarrow$ index sets $\mathcal{I}_k$ $(k = 2, \cdots, K)$
6: **output:** IP $\mathcal{P} = \{\mathbf{a}_i \,|\, i \in \mathcal{I}_0 = \mathcal{I}_1 \cup \cdots \cup \mathcal{I}_K\}$

[5] In practice, we can use other information (e.g., UE locations) to determine a small subset of $\mathcal{F}$, which can further reduce the training overhead.

Note that in Algorithm 3 (and Algorithm 1), it is implicitly assumed that channel covariance matrix and PAS change slowly, which has been verified. In fact, they are typical long-term information and have been widely exploited [6], [7]. In Algorithm 3, once an IP is available, we can use it to acquire instantaneous PSI and further design precoders. In a long time, there is no need to acquire an IP again.

B. Optimal IP Design via Contextual Bandit Learning

Next, we tackle the issue of finding an optimal regularization parameter $\rho^\star$. The selection of ρ is important. If ρ is set too large, important mCSI is not effectively captured and fully exploited, which inevitably leads to a bad performance. On the other hand, if ρ is set too small, the IP is not sparse, which leads to large training and feedback overheads. Since the optimal $\rho^\star$ depends on many factors (e.g., transmit power, QoS requirement, external environments, and so on), it is very difficult to derive an analytical selection criterion.

Next, we propose a learning-based solution to tackle this issue. More specifically, we employ contextual bandit (CB) learning to design an efficient algorithm. CBs are lightweight reinforcement learning (RL) problems which have no persistent state. At each step, the BS (i.e., agent in RL) is presented with a context X and a choice of one of several possible actions a. Since different actions yield different unknown rewards, the BS shall choose the action that yields the highest expected reward. The reader is referred to [42] for more details of CB.

The core of employing CB is to formulate the problem of interest (e.g., parameter optimization in this paper) as a CB problem, namely to define rewards, contexts, action space and bandit model. To reduce computational complexity, the time-scale of optimizing the learning module is larger than that of the precoding module, i.e., the learning module is optimized every $K(K>1)$ time-slots (which is referred to as a time-unit) while the precoder is updated each time-slot. The details of the problem formulation are as follows.

1) Action Space: To obtain an appropriate value of ρ, it is initialized by a random or fixed value (e.g., $\rho=10.0$). Then, during the process of learning, it is adjusted to an appropriate value. The action space is defined by a set of constants

$$\mathcal{A}=\{a_1>0, a_2>0, \cdots, a_{|\mathcal{A}|}>0\}, \tag{29}$$

which indicate to increase or decrease the value of ρ. If the value of ρ in time-unit t is ρ_t and $a_i\in\mathcal{A}$ is chosen, then the value of ρ in time-unit $t+1$ is $\rho_{t+1}=a_i\rho_t$.

2) Rewards: The reward r is often a PMoI. Since the focus of this paper is SLP, the reward can be a linear combination of symbol error rate (SER), transmit power, training overhead, and feedback overhead. In this paper, the reward is defined as a linear combination of the SER and training overhead, i.e.,

$$r_t=-C\log(\max\{b_t,c_0\})-|\mathcal{P}|, \tag{30}$$

where $C>0$ is a constant (introduced to adjust the dynamic range of the rewards), b_t is the SER at time-unit t, and $|\mathcal{P}|$ (the size or cardinality of the pilot $\mathcal{P}$) characterizes the training overhead. Since the SER may be zero, a small value $c_0>0$ is introduced in (30) to avoid the invalid value ∞.

3) Contexts: The context X_t reflects important states and/or changes of the communication system. It consists of elements that affect the system PMoI. Let X_t' represent the system state in time-unit t, which is defined as

$$X_t'=\Big(\|\hat{\mathbf{h}}_1\|_2,\cdots,\|\hat{\mathbf{h}}_U\|_2,\|\hat{\mathbf{h}}_1\|_0,\cdots,\|\hat{\mathbf{h}}_U\|_0, \gamma_1,\cdots,\gamma_U,\|\mathbf{d}\|_2\Big), \tag{31}$$

where $\{\|\hat{\mathbf{h}}_u\|_0\}$ are included to measure pilot overhead. The context X_t is defined by c successive system states, i.e.,

$$X_t=(X_t',X_{t-1}',\cdots,X_{t-c+1}'). \tag{32}$$

The reason that the contexts are defined by successive system states is that each single state only describes static properties of the system. However, the decisions (i.e., to increase/decrease ρ) are made according to the changes of the system.

To complete CB modeling, we need to build a model $r(X,a)$ of distribution of the rewards conditioned on the context and action. With this model available, the BS can choose actions. In view that the communication environment is often dynamic and complex and simple models (e.g., linear model) are insufficient to make wise decisions because of the limited representative power, neural networks (NNs), which are sufficiently flexible, are considered here. Then, the model can be denoted by $r(X,a|\mathbf{w})$, where $\mathbf{w}$ represents the parameters of the NN (i.e., the weights and biases). The details of the NN (i.e., input, output and loss function) are as follow:

- Network structure: Without loss of generality, the commonly used forward/fully-connected NN is considered for simplicity. The number of neurons of the output layer is $|\mathcal{A}|$, i.e., the size of the action space $\mathcal{A}$.
- Input and output: The input and output of the NN are the contexts and rewards, respectively. The output of the NN is of dimension $|\mathcal{A}|$, and the i-th neuron of the output layer predicts the reward corresponding to action i.
- Loss function: Let X and $\mathrm{NNet}(X)$ represent the input and output of the NN. The loss function is the square of the $L2$ distance, i.e., $\|\mathbf{y}-\mathrm{NNet}(X)\|^2$, where $\mathbf{y}$ (of dimension $|\mathcal{A}|$) is the label output corresponding to X. [6]

A fundamental issue of bandit learning is to balance the tradeoff between exploitation (to pick the best known action) and exploration (to pick potentially sub-optimal exploratory actions). However, the previous model is deterministic, based on which it is difficult to derive a good policy that well deals with the dilemma of exploration and exploitation. To tackle this issue, the Bayes idea is incorporated into the NN, which yields the Bayesian NN (BNN) [43]. Specifically, all weights and biases of the BNN are represented by probability distributions over possible values, rather than having a single fixed value. BNN can represent uncertainties intrinsically. Instead of training a single network, an ensemble of infinite networks are trained. To obtain a BNN, we place a prior $P(\mathbf{w})$

[6]The label output is constructed as follows. In the CB problem (and also all bandit problems), given a context X, one and only one action can be picked. Hence, if an action $a_i\in\mathcal{A}$ is chosen and the resultant reward is r_i, the label output corresponding to X and a_i is constructed as $\mathbf{y}=[\mathbf{0}_{i-1},r_i,\mathbf{0}_{|\mathcal{A}|-i}]$, i.e., the i-th component is r_i and the other components are zero.

on $\mathbf{w}$, and the prior $P(\mathbf{w})$ is updated into a posterior $P(\mathbf{w}|\mathcal{D})$ when a training dataset $\mathcal{D}$ is available. However, due to a large number of parameters and the complex functional form of the NN, an exact inference of the posterior $P(\mathbf{w}|\mathcal{D})$ is intractable.

Fortunately, although an exact inference is intractable, an approximate solution to $P(\mathbf{w}|\mathcal{D})$ obtained via variational inference (VI) often meets practical requirement [43]. VI is a powerful approximate inference approach, which has been widely used in machine learning and signal processing [44]. As a deterministic approximate inference technique, the basic idea of VI is to pick an approximation to the distribution of interested from some tractable distribution family, and then to try to make this approximation as close as possible to the true posterior $P(\mathbf{w}|\mathcal{D})$. This reduces an intractable inference problem to a tractable optimization problem.

Let $\{Q(\mathbf{w}|\boldsymbol{\xi})\}$ be a distribution family parameterized by $\boldsymbol{\xi}$. Similar to [43], diagonal Gaussian distribution family is chosen in this paper, i.e., $\boldsymbol{\xi}$ incorporates mean and variance vectors. Specifically, $\mathbf{w}$ is distributed as $\mathbf{w} \sim \mathcal{CN}(\boldsymbol{\mu}, \boldsymbol{\Lambda})$, where $\boldsymbol{\mu}$ and $\boldsymbol{\Lambda}$ (a diagonal matrix) are mean and variance vectors, respectively. The Kullback-Leibler (KL) divergence is often utilized to measure the distance between two distributions. To transform the inference problem into an optimization problem, VI tries to find the optimal parameter $\boldsymbol{\xi}^\star$ by minimizing the KL divergence between the variational distribution and the true Bayesian posterior $P(\mathbf{w}|\mathcal{D})$, i.e.,

$$\begin{aligned}\boldsymbol{\xi}^\star &= \arg\min_{\boldsymbol{\xi}} \mathrm{KL}(Q(\mathbf{w}|\boldsymbol{\xi})\|P(\mathbf{w}|\mathcal{D})) \\ &= \arg\min_{\boldsymbol{\xi}} \int Q(\mathbf{w}|\boldsymbol{\xi}) \log\left(\frac{Q(\mathbf{w}|\boldsymbol{\xi})}{P(\mathbf{w})P(\mathcal{D}|\mathbf{w})}\right) \\ &= \arg\min_{\boldsymbol{\xi}} \mathrm{KL}(Q(\mathbf{w}|\boldsymbol{\xi})\|P(\mathbf{w})) - \mathbb{E}_{Q(\mathbf{w}|\boldsymbol{\xi})}[\log P(\mathcal{D}|\mathbf{w})].\end{aligned}$$

Equivalently, the loss function to train the NN is given by

$$\mathrm{KL}(Q(\mathbf{w}|\boldsymbol{\xi})\|P(\mathbf{w})) - \mathbb{E}_{Q(\mathbf{w}|\boldsymbol{\xi})}[\log P(\mathcal{D}|\mathbf{w})]. \tag{33}$$

Before proceeding to details of optimizing ρ via learning, we first point out how to compute the loss in (33). The calculation of the first term, i.e., $\mathrm{KL}(Q(\mathbf{w}|\boldsymbol{\xi})\|P(\mathbf{w}))$, depends on the assumptions on Q and P, which, in general, cannot be computed analytically. To simplify the calculation (typically, to compute it analytically), the prior $P(\mathbf{w})$ is simply set to be $\mathcal{N}(\mathbf{0}, \mathbf{I})$ in Section V of this paper. Similarly, the diagonal Gaussian distribution is chosen as the variational posterior, i.e., $Q(\mathbf{w}|\boldsymbol{\xi}) = \mathcal{N}(\boldsymbol{\zeta}, \boldsymbol{\Lambda})$, where $\boldsymbol{\zeta}$ and $\boldsymbol{\Lambda}$ are the mean vector and covariance matrix (a diagonal matrix), respectively. Then, $\mathrm{KL}(Q(\mathbf{w}|\boldsymbol{\xi})\|P(\mathbf{w}))$ can be analytically calculated as

$$\begin{aligned}&\mathrm{KL}(Q(\mathbf{w}|\boldsymbol{\xi})\|P(\mathbf{w})) \\ =&0.5\big(\mathrm{tr}(\boldsymbol{\Lambda}) + \boldsymbol{\zeta}^{\mathrm{T}}\boldsymbol{\zeta} - \log\det(\boldsymbol{\Lambda}) - d\big),\end{aligned} \tag{34}$$

where d denotes the dimension of $\mathbf{w}$. As for the second term, i.e., $\mathbb{E}_{Q(\mathbf{w}|\boldsymbol{\xi})}[\log P(\mathcal{D}|\mathbf{w})]$, it can be estimated via the Monte-Carlo sampling.

Now, we can present an efficient algorithm to find $\rho^\star$. The designed algorithm is based on the Thompson sampling (TS) [42]. The basic idea of TS is to choose an action to play according to its probability of being the best action. At each step, TS draws a new set of parameters and then picks the action relative to those parameters. This can be seen as a kind of stochastic hypothesis testing: more probable parameters are drawn more often and thus refuted or confirmed the fastest. TS repeats the following operations: (1) sample a new set of parameters for the model; (2) choose the action with the highest expected reward according to the sampled parameters; (3) update the model and goto step (1). Please refer to [42] for more details of TS. For clarity, the algorithm that incorporates both parameter optimization and IP search is summarized in Algorithm 4.

Algorithm 4: Environment-Sensing IP via CB Learning

1: **input:** action space $\mathcal{A} = \{a_1, a_2, \cdots, a_{|\mathcal{A}|}\}$; update frequency of NN F; number of successive states c

2: **initialize** prior $P(\mathbf{w})$; experience memory $\mathcal{D} = \emptyset$; regularization parameter ρ_0; let $t = 1$

3: **repeat** for each time-unit

(a) construct context X_t according to (31) and (32)

(b) sample $P(\mathbf{w}|\mathcal{D}) \Longrightarrow$ NN parameters $\mathbf{w}'$

(c) compute $\mathbf{y} = \mathrm{NNet}(X_t)$ with input X and NN parameters $\mathbf{w}'$

(d) find out optimal action $a_t^\star$ with $a_t^\star$ given by $a_t^\star = \arg\max_{a\in\mathcal{A}}\{y_a \,|\, a = 1, \cdots, |\mathcal{A}|\}$

(e) update value of ρ, i.e., $\rho_t = a_t^\star \rho_{t-1}$

(f) invoke Algorithm 3 to search IP

(g) receive reward r_t (from external environment)

(h) update memory $\mathcal{D}$: $\mathcal{D} \leftarrow \mathcal{D}\bigcup\{(X_t, a_t^\star, r_t)\}$

(i) if $t \bmod F = 0$, update NN via VI with $\mathcal{D}$

(j) let $t \leftarrow t + 1$

end

To use the algorithm, we need to construct an action space $\{a_1, \cdots, a_{|\mathcal{A}|}\}$. Then, we initialize the prior of the parameters $\mathbf{w}$ of the underlying NN. For simplicity, the prior placed on $\mathbf{w}$ is given by $\mathbf{w} \sim \mathcal{CN}(\mathbf{0}, \sigma_{\mathbf{w}}^2\mathbf{I})$ with $\sigma_{\mathbf{w}}^2$ a constant. The experience memory is emptied and the counter is set to 1. Next, in each time-unit we repeat the following operations. In step (a), the context X_t is constructed based on the information collected within c successive time-units up to t. In step (b), the concrete parameters $\mathbf{w}'$ and thus a concrete NN are obtained by sampling the posterior $P(\mathbf{w}|\mathcal{D})$. Since the posterior is unavailable at the beginning stage (e.g., $t = 1$), the prior $P(\mathbf{w})$ can be used instead. By feeding X_t to the NN, the predicted expected rewards, the picked action $a_t^\star$ and regularization parameter ρ_t can be obtained in steps (c), (d) and (e), respectively. With $\rho_t^\star$ available, the IP search method in Algorithm 3 can be invoked in step (f). The BS receives the reward from the external environment and updates the memory in steps (g) and (h), respectively. In step (i), with sufficient experiences available, the NN can be updated. At the end of each time-unit, the counter is increased by 1.

V. Simulation Results

In this section, simulation results are provided to demonstrate the performance of the proposed algorithms. Without loss of generality, the uniform linear array is considered. Two types of typical PAS functions are chosen to evaluate different algorithms, i.e., PAS with the uniform distribution denoted by

$S_{\text{uni}}(\theta)$ and PAS with the Laplacian distribution denoted by $S_{\text{lap}}(\theta)$ [7], which are respectively given by

$$S_{\text{uni}}(\theta) = \frac{1}{2\Delta}, \quad \forall\, \theta \in [\bar{\theta} - \Delta, \bar{\theta} + \Delta], \tag{35}$$

$$S_{\text{lap}}(\theta) = \frac{1}{\sqrt{2}\Delta} e^{-\sqrt{2}|\theta - \bar{\theta}|/\Delta}. \tag{36}$$

During the process of estimating PSI and feeding it back to the BS, it is inevitable to incur two types of noise, i.e., the Gaussian noise (when estimating the PSI) and the quantization noise (when quantizing the PSI). Let $\hat{\mathbf{h}}_u$ denote the estimation of accurate mCSI $\mathbf{h}_u$. Similar to [25] and for simplicity, $\hat{\mathbf{h}}_u$ and $\mathbf{h}_u$ are assumed to satisfy

$$\mathbf{h}_u = \hat{\mathbf{h}}_u + \Delta\mathbf{h}_u^{\text{G}} + \Delta\mathbf{h}_u^{\text{Q}}, \tag{37}$$

where $\Delta\mathbf{h}_u^{\text{G}}$ and $\Delta\mathbf{h}_u^{\text{Q}}$ denote the Gaussian noise and quantization noise, respectively. $\Delta\mathbf{h}_u^{\text{G}}$ is distributed as $\mathcal{CN}(0, \sigma_g^2\mathbf{I})$, while the distribution of $\Delta\mathbf{h}_u^{\text{Q}}$ depends on the quantization method and the number of quantization bits. The simplest uniform element-wise scalar quantization method is chosen in this paper. The real part and imaginary part of a complex number are quantized independently. The number of quantization bits (to quantize a real number) is denoted by Q.

For comparison, the fully-digital SLP (FD-SLP) solution of [25] and the fully-sweeping SLP (FS-SLP) solution in [36] (with some modifications) are chosen as benchmarks to evaluate the algorithms proposed in this paper. Note that the FD-SLP algorithm requires the (complete) pCSI, i.e., $\bar{\mathbf{h}}_u$ in (1), to design a precoder, while the FS-SLP algorithm requires the complete mCSI, i.e., $\{\mathbf{F}^{\text{H}}\bar{\mathbf{h}}_u\}$, to design a precoder. Also, for the pCSI, the relationship between $\bar{\mathbf{h}}_u$ (perfect pCSI) and $\hat{\bar{\mathbf{h}}}_u$ (estimated pCSI) takes a similar form in (37).

SER, total transmit power, training/feedback overhead and throughput are chosen as performance metrics to evaluate different algorithms. For the sake of convenience, the joint pilot and symbol-level precoding (JoPiSLP) algorithms in this paper with the IPs constructed based on the PAS support directly, by using the SMB technique and the contextual bandit learning (CBL) method (in Algorithms 3 and 4) are named as JoPiSLP-PAS, JoPiSLP-SMB and JoPiSLP-CBL, respectively. Default parameters/settings (e.g., modulation mode) shared by relevant algorithms are provided in Table I.

TABLE I
DEFAULT PARAMETERS SHARED BY RELEVANT ALGORITHMS

Parameter	Value
Number of Served Users	$U = 3$
Number of Transmit Antennas	$N = 64$
PAS Support of User 1	$[-33/64, -27/64]$
PAS Support of User 2	$[-3/64, 3/64]$
PAS Support of User 3	$[27/64, 33/64]$
Modulation Mode (or Constellation)	QPSK
Number of States to Construct Context	$c = 2$
Update Frequency of NN	$F = 10$

Firstly, we demonstrate that the mCSI-ISS technique helps to achieve a scalable tradeoff between a desired performance metric and the training overhead (measured via the length of IP), by adjusting the value of ρ in (25) and using Algorithm 3. As shown in Fig. 3-(a), it is observed that as the parameter ρ increases the length of IP reduces. It can be observed from Fig. 3-(b) that even though the available training overhead is low (e.g., the length of IP is equal to 6), a relatively good SER performance can still be achieved. One can also observe that as the training overhead declines, the SER performance first becomes better and then becomes worse. The reason for this is as follows. Since the estimated mCSI is inaccurate, the use of less inaccurate (but significant) mCSI to design a precoder implies that the noise amplification effect is smaller. Hence, as the length of IP reduces, the SER performance first becomes better. However, if the length of IP is too small, very limited significant mCSI can be captured. As a result, the SER performance becomes worse as the length of IP further reduces, which coincides with our intuitions.

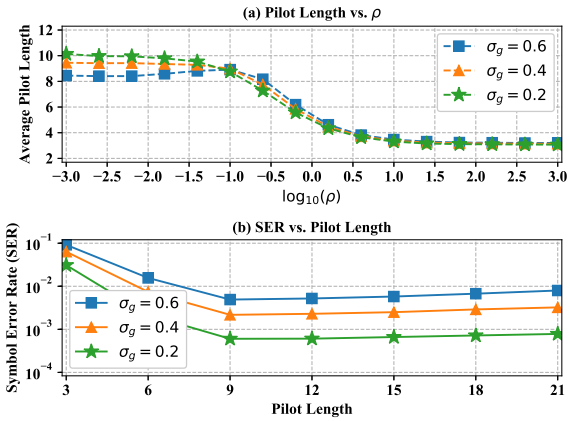

Fig. 3. The length of IP versus parameter ρ and the tradeoff between the SER performance and the length of IP: $Q = 8$, $\gamma_u = 6$dB and $S_{\text{lap}}(\theta)$.

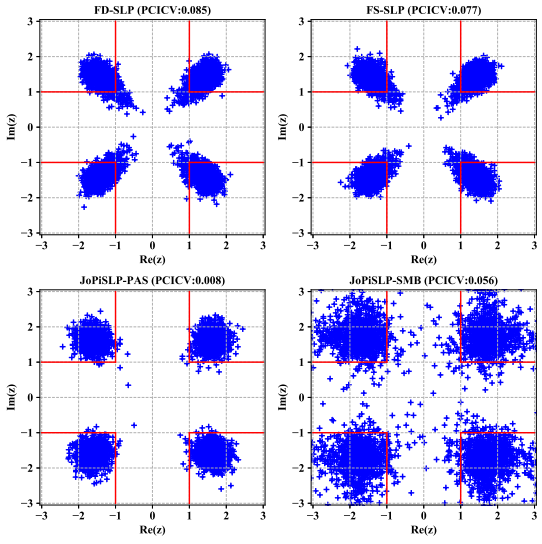

Fig. 4. Constellations (i.e., noise-free received signals) of different SLP algorithms: $\gamma_u = 3$dB, $Q = 6$, $\sigma_g = 0.3$ and $S_{\text{uni}}(\theta)$. "PCICV" is referred to as probability of CI constraint violation, i.e., the probability that the noise-free received signals are located in region $\{z \,|\, 1 \geq |\text{Re}(z)| \text{ or } 1 \geq |\text{Im}(y)|\}$.

Next, we evaluate the two heuristic algorithms proposed in

this paper (i.e., JoPiSLP-PAS and JoPiSLP-SMB) and confirm the robustness of the IP approach. To demonstrate the advantages of the IP-based algorithms intuitively, the constellations (i.e., noise-free received signals) of different algorithms are shown in Fig. 4. It is seen that the noise-free received signals are roughly located in a semi-infinite rectangular region (i.e., taking the form $\{z \,|\, x_0 \leq |\mathrm{Re}(z)|, y_0 \leq |\mathrm{Im}(y)|\}$ [7]). This attributes to the CI constraints, which force the received signals to be away from the decision boundaries. It is also observed from Fig. 4 that for both JoPiSLP-PAS and JoPiSLP-SMB, less points are located in region $\{z \,|\, 1 \geq |\mathrm{Re}(z)| \text{ or } 1 \geq |\mathrm{Im}(y)|\}$ (or close to the coordinate axes). The reason for this is that only a part (but the most important part) of mCSI is sensed and used by JoPiSLP-PAS and JoPiSLP-SMB to design precoders, while the complete pCSI or mCSI is used by FD-SLP or FS-SLP to design precoders. However, since the pCSI and mCSI are inaccurate in this case, if less of them are used, the degree that the CI constraints are violated becomes smaller. Note that if the noise-free received signals are more close to the axes, they are more vulnerable to the noise. Therefore, it is expected that a better SER performance can be achieved by JoPiSLP-PAS and JoPiSLP-SMB, as shown in Fig. 5.

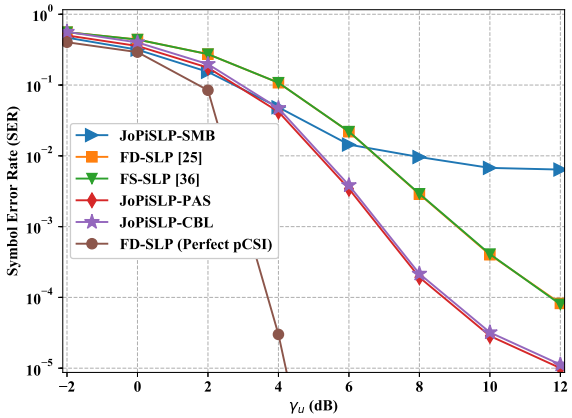

Fig. 5. The SER performance of different SLP algorithms: $Q = 8$, $\sigma_g = 0.4$ and $S_{\text{uni}}(\theta)$.

TABLE II
TRAINING AND FEEDBACK OVERHEADS (NORMALIZED TO FS-SLP)

Algorithm	Training Overhead	Feedback Overhead
FD-SLP	1.0	1.0
FS-SLP	1.0	1.0
JoPiSLP-PAS	0.406	0.406
JoPiSLP-SMB	0.188	0.188
JoPiSLP-CBL	0.375	0.375

To show that the superiorities of the proposed approaches still hold for more general channel models, the PAS support of UE 3 has been modified as $[27/64, 33/64] \cup [41/64, 45/64]$, i.e., the channel consists of two clusters and thus has larger AS. The SER performance of different SLP algorithms is shown in Fig. 5. The training and feedback overheads are compared in Table II [8]. It is not surprising that FD-SLP with perfect pCSI achieves the best SER performance. However, the SER performance achieved by FD-SLP (or FS-SLP) with inaccurate pCSI (or inaccurate and complete mCSI) is worse than that achieved by JoPiSLP-PAS. The reason for this is two-fold. On the one hand, significant mCSI is captured by the constructed IP. On the other hand, insignificant inaccurate mCSI is discarded, which alleviates the noise amplification effect. Besides the good SER performance, another important advantage of JoPiSLP-PAS is that both training and feedback overheads of JoPiSLP-PAS are much less than those of FD-SLP and FS-SLP, which is very appealing for FDD systems.

Interestingly, it is observed from Fig. 5 that JoPiSLP-SMB achieves a better SER performance than both FD-SLP and FS-SLP when $\{\gamma_u\}$ are relatively small (i.e., $\gamma_u < 7$dB). However, when $\gamma_u > 7$dB, the SER performance curve becomes flat. The reason for this is that the use of the SMB technique incurs more interferences. In fact, each pilot beam in $\mathcal{P}'_\theta$ corresponds to multiple beams, and thus the interferences caused by the sidelobes of other beams within the pilot beam further reduce the accuracy of the obtained PSI. However, the advantage of the SMB IP $\mathcal{P}'_\theta$ is that compared to the PAS IP $\mathcal{P}_\theta$, the training and feedback overheads have been further reduced. Moreover, when σ_g is relatively small, the achieved SER performance can often meet practical requirements.

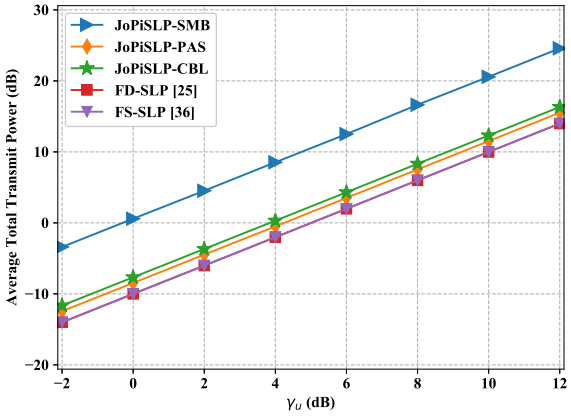

Fig. 6. Average total transmit power required by different SLP algorithms: $Q = 8$, $\sigma_g = 0.4$ and $S_{\text{uni}}(\theta)$.

The performance in terms of average total transmit power required by different SLP algorithms is shown in Fig. 6. It is seen that compared to FD-SLP and FS-SLP, JoPiSLP-PAS requires a bit more transmit power for the same γ_u setting. The reason for this is that less (equivalent or virtual) antennas are used by JoPiSLP-PAS, which leads to a small loss of channel power. More specifically, in contrast to FD-SLP (or FS-SLP),

[7]The reason for taking this form is due to the QPSK modulation. [25]

[8]Compared to instantaneous CSI/mCSI that changes every time-slot, PAS is a long-term quantity and varies very slow. Hence, the overheads of training and feedback caused by beam space sweeping dominate, and the overheads of acquiring and feeding back PAS information can be omitted. Since the training overhead is proportional to the number of beams used for sweeping beam space and the number of beams used by FS-SLP is equal to the size of the codebook, the training overhead is measured by normalizing to FS-SLP. Similarly, since the feedback overhead is proportional to the number of used beams, the feedback overhead is also measured by normalizing to FS-SLP.

where all components of each $\bar{\mathbf{h}}_u$ (or each $\mathbf{h}_u = \mathbf{F}^{\mathrm{H}}\bar{\mathbf{h}}_u$) are utilized, only a part of the components of each $\mathbf{h}_u$ are used to design precoders, while other components are discarded. As a result, to obtain the same performance, more transmit power is required to compensate for the channel power loss. It is also observed that for JoPiSLP-SMB it costs much more transmit power to achieve the same performance. The reason for this is that much less PSI is used by JoPiSLP-SMB and the used PSI is more inaccurate due to the multiple-beam interferences, which thus requires more transmit power to compensate for the loss. From the above discussion, we can conclude that the proposed IP approach can achieve a good tradeoff between transmit power and a desired performance metric.

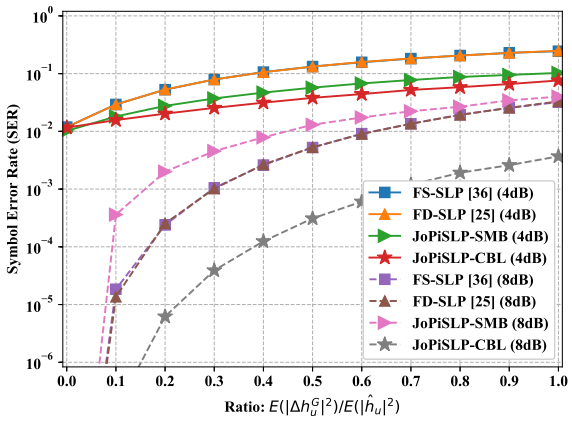

Fig. 7. The SER performance of different SLP algorithms under various degrees of CSI uncertainties: $Q = 8$ and $S_{\mathrm{lap}}(\theta)$. Note that "4dB" and "8dB" correspond to the settings $\gamma_u = 4$dB and $\gamma_u = 8$dB, respectively.

Fig. 7 further shows the SER performance of different SLP algorithms under various degrees of CSI uncertainties. It is seen that for the low SNR setting (i.e., $\gamma_u = 4$dB), JoPiSLP-SMB achieves a better performance than FD-SLP and FS-SLP. However, for the high SNR setting (i.e., $\gamma_u = 8$dB), both FD-SLP and FS-SLP perform better than JoPiSLP-SMB. The reason for this is that due to the multiple-beam interferences, the PSI used by JoPiSLP-SMB is less accurate. One can also observe that for the two SNR settings, JoPiSLP-CBL performs much better than the other algorithms. The reason for this is that JoPiSLP-CBL can automatically sense required PSI and acquire it with the minimal training and feedback cost.

One of the most important advantages of the IP approach is that it is feedback-efficient. It is assumed that each communication frame consists of L_{T} time-slots and within each time-slot N_{U} (or N_{D}) bits can be transmitted via the uplink (or downlink) channel. If N_{F} bits are used to feed back the PSI to the BS, the number of available time-slots to transmit effective data is $L_{\mathrm{T}} - \lceil N_{\mathrm{F}}/N_{\mathrm{U}} \rceil$. In general, if more bits are allocated for feeding back the PSI to the BS, the PSI is more accurate. However, less time-slots can be used to transmit effective data. Throughput is chosen as the performance metric to evaluate different algorithms [20], which is defined as

$$C = mU(1 - \mathrm{BLER})(1 - \lceil N_{\mathrm{F}}/N_{\mathrm{U}} \rceil / L_{\mathrm{T}}), \qquad (38)$$

where BLER represents the block error rate [20], $m = \log_2 M$ denotes the bit information per symbol for MPSK modulation, and $1 - \lceil N_{\mathrm{F}}/N_{\mathrm{U}} \rceil / L_{\mathrm{T}}$ is included to incorporate the feedback overhead.

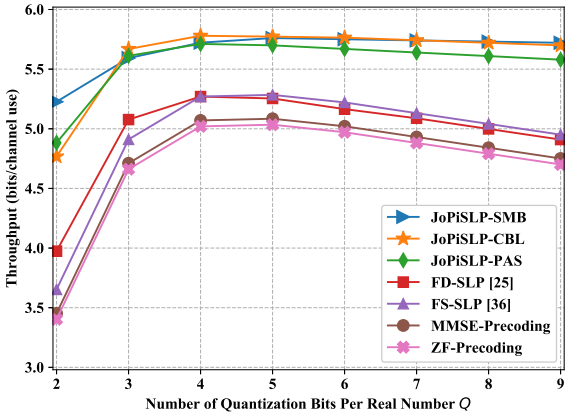

Fig. 8. Average throughput vs. Q for different SLP algorithms: $\sigma_g = 0.24$, $\gamma_u = 4$dB, $L_{\mathrm{T}} = 256$, $N_{\mathrm{U}} = 32$, $N_{\mathrm{D}} = 128$ and $S_{\mathrm{uni}}(\theta)$.

Fig. 8 shows the throughput performance of different SLP algorithms under various numbers of quantization bits per real number. It is observed that as Q (the number of quantization bits per real number) increases, the throughput first increases and then declines. The reason for this is that as Q increases, the obtained PSI becomes more accurate and thus the BLER performance becomes better. Note that the increase of Q implies that less time resources are reserved for transmitting effective data. Therefore, when the PSI is sufficiently accurate, the increase of Q, on the contrary, deteriorates the final throughput performance. It is not surprising that the IP-based algorithms perform better than the other two algorithms, because the IP-based algorithms are both training- and feedback-efficient. It is also observed that the SLP-based precoding methods achieve a better throughput performance than the classical MMSE and ZF precoding methods. In fact, it has already been established in the literature [22]–[25] that SLP greatly outperforms conventional precoding schemes.

VI. Conclusion

For the FDD downlink multi-user system, we proposed a unified precoding and pilot design optimization framework, aiming to reduce the overheads of training and feedback. We first showed that CSI acquisition and precoding optimization can be jointly designed, without estimating and reconstructing the pCSI. We further proposed to employ training- and feedback-efficient IPs to sense and capture PSI, based on which the precoders can be optimized directly. Then, we proposed two heuristic IP construction methods. To enhance the heuristic methods, we further proposed a learning-based IP design algorithm. The learning-based algorithm not only improves the system performance, but also avoids estimating the PAS information. Finally, simulation results confirmed the effectiveness and superiority of our proposal.

APPENDIX A
PROOF OF THEOREM 1

Note that since $\mathcal{F}$ spans the linear space $\mathbb{C}^N$, for an arbitrary solution $\{\mathbf{v}_w\}$ of problem (7), there exists at least one $\mathbf{y}_w$ such that $\mathbf{v}_w = \mathbf{F}\mathbf{y}_w$ holds true for each $\mathbf{v}_w$, i.e., the set $\{\mathbf{y}_w\}$ is a solution of problem (9). Conversely, for an arbitrary solution $\{\mathbf{y}_w\}$ of problem (9), it can be verified directly that the set $\{\mathbf{F}\mathbf{y}_w\}$ is a solution of problem (7). In particular, if the set $\{\mathbf{y}_w^\star\}$ is an optimal solution of problem (9), the set $\{\mathbf{v}_w^\star = \mathbf{F}\mathbf{y}_w^\star\}$ is an optimal solution of problem (7). In fact, for an arbitrary solution $\{\mathbf{v}_w'\}$ of problem (7), there exists a set $\{\mathbf{y}_w'\}$ such that $\{\mathbf{v}_w' = \mathbf{F}\mathbf{y}_w'\}$ hold true. The optimality of $\{\mathbf{y}_w^\star\}$ with respect to $\{\mathbf{y}_w'\}$, along with the relationship (or form) between problems (7) and (9), implies the optimality of $\{\mathbf{v}_w^\star\}$ with respect to $\{\mathbf{v}_w'\}$, which completes the proof.

REFERENCES

[1] E. G. Larsson, O. Edfors, F. Tufvesson, and T. L. Marzetta, "Massive MIMO for next generation wireless systems," *IEEE Commun. Mag.*, vol. 52, no. 2, pp. 186–195, 2014.

[2] F. Rusek, D. Persson, B. K. Lau, E. G. Larsson, T. L. Marzetta, O. Edfors, and F. Tufvesson, "Scaling up MIMO: Opportunities and challenges with very large arrays," *IEEE Signal Process. Mag.*, vol. 30, no. 1, pp. 40–60, 2013.

[3] Y. Han, Q. Liu, C. Wen, S. Jin, and K. Wong, "FDD massive MIMO based on efficient downlink channel reconstruction," *IEEE Trans. Commun.*, vol. 67, no. 6, pp. 4020–4034, 2019.

[4] X. Rao and V. K. N. Lau, "Distributed compressive csit estimation and feedback for FDD multi-user massive MIMO systems," *IEEE Trans. Signal Process.*, vol. 62, no. 12, pp. 3261–3271, 2014.

[5] M. E. Eltayeb, T. Y. Al-Naffouri, and H. R. Bahrami, "Compressive sensing for feedback reduction in MIMO broadcast channels," *IEEE Trans. Commun.*, vol. 62, no. 9, pp. 3209–3222, 2014.

[6] A. Adhikary, J. Nam, J. Ahn, and G. Caire, "Joint spatial division and multiplexing - the large-scale array regime," *IEEE Trans. Inf. Theory*, vol. 59, no. 10, pp. 6441–6463, 2013.

[7] H. Xie, F. Gao, S. Jin, J. Fang, and Y. Liang, "Channel estimation for TDD/FDD massive MIMO systems with channel covariance computing," *IEEE Trans. Wireless Commun.*, vol. 17, no. 6, pp. 4206–4218, 2018.

[8] K. Hugl, J. Laurila, and E. Bonek, "Downlink beamforming for frequency division duplex systems," in *Proc. IEEE GLOBECOM*, vol. 4, Dec. 1999, pp. 2097–2101 vol.4.

[9] A. Decurninge, M. Guillaud, and D. T. M. Slock, "Channel covariance estimation in massive MIMO frequency division duplex systems," in *2015 IEEE Globecom Workshops (GC Wkshps)*, 2015, pp. 1–6.

[10] J. Fang, X. Li, H. Li, and F. Gao, "Low-rank covariance-assisted downlink training and channel estimation for FDD massive MIMO systems," *IEEE Trans. Wireless Commun.*, vol. 16, no. 3, pp. 1935–1947, 2017.

[11] Y. Yang, F. Gao, Z. Zhong, B. Ai, and A. Alkhateeb, "Deep transfer learning-based downlink channel prediction for FDD massive mimo systems," *IEEE Trans. Commun.*, vol. 68, no. 12, pp. 7485–7497, 2020.

[12] C. Wen, W. Shih, and S. Jin, "Deep learning for massive MIMO CSI feedback," *IEEE Wireless Commun. Lett.*, vol. 7, no. 5, pp. 748–751, 2018.

[13] J. Guo, C. Wen, S. Jin, and G. Y. Li, "Convolutional neural network-based multiple-rate compressive sensing for massive MIMO CSI feedback: Design, simulation, and analysis," *IEEE Trans. Wireless Commun.*, vol. 19, no. 4, pp. 2827–2840, 2020.

[14] F. Sohrabi and W. Yu, "Hybrid digital and analog beamforming design for large-scale antenna arrays," *IEEE J. Sel. Topics Signal Process.*, vol. 10, no. 3, pp. 501–513, 2016.

[15] X. Gao, L. Dai, S. Han, C. I, and R. W. Heath, "Energy-efficient hybrid analog and digital precoding for mmwave MIMO systems with large antenna arrays," *IEEE J. Sel. Areas Commun.*, vol. 34, no. 4, pp. 998–1009, 2016.

[16] X. Yu, J. Shen, J. Zhang, and K. B. Letaief, "Alternating minimization algorithms for hybrid precoding in millimeter wave MIMO systems," *IEEE J. Sel. Topics Signal Process.*, vol. 10, no. 3, pp. 485–500, 2016.

[17] J. Zhang, Y. Huang, J. Wang, and L. Yang, "Hybrid precoding for wideband millimeter-wave systems with finite resolution phase shifters," *IEEE Trans. Veh. Technol.*, vol. 67, no. 11, pp. 11 285–11 290, Nov 2018.

[18] Y. Huang, J. Zhang, and M. Xiao, "Constant envelope hybrid precoding for directional millimeter-wave communications," *IEEE J. Sel. Areas Commun.*, vol. 36, no. 4, pp. 845–859, April 2018.

[19] C. Masouros and E. Alsusa, "Dynamic linear precoding for the exploitation of known interference in MIMO broadcast systems," *IEEE Trans. Wireless Commun.*, vol. 8, no. 3, pp. 1396–1404, 2009.

[20] C. Masouros, "Correlation rotation linear precoding for MIMO broadcast communications," *IEEE Trans. Signal Process.*, vol. 59, no. 1, pp. 252–262, 2011.

[21] C. Masouros and T. Ratnarajah, "Interference as a source of green signal power in cognitive relay assisted co-existing MIMO wireless transmissions," *IEEE Trans. Commun.*, vol. 60, no. 2, pp. 525–536, 2012.

[22] C. Masouros, T. Ratnarajah, M. Sellathurai, C. B. Papadias, and A. K. Shukla, "Known interference in the cellular downlink: a performance limiting factor or a source of green signal power?" *IEEE Commun. Mag.*, vol. 51, no. 10, pp. 162–171, 2013.

[23] C. Masouros, M. Sellathurai, and T. Ratnarajah, "Vector perturbation based on symbol scaling for limited feedback MISO downlinks," *IEEE Trans. Signal Process.*, vol. 62, no. 3, pp. 562–571, 2014.

[24] M. Alodeh, S. Chatzinotas, and B. Ottersten, "Constructive multiuser interference in symbol level precoding for the MISO downlink channel," *IEEE Trans. Signal Process.*, vol. 63, no. 9, pp. 2239–2252, 2015.

[25] C. Masouros and G. Zheng, "Exploiting known interference as green signal power for downlink beamforming optimization," *IEEE Trans. Signal Process.*, vol. 63, no. 14, pp. 3628–3640, 2015.

[26] E. Alsusa and C. Masouros, "Adaptive code allocation for interference management on the downlink of DS-CDMA systems," *IEEE Trans. Wireless Commun.*, vol. 7, no. 7, pp. 2420–2424, 2008.

[27] C. Masouros and E. Alsusa, "Two-stage transmitter precoding based on data-driven code-hopping and partial zero forcing beamforming for MC-CDMA communications," *IEEE Trans. Wireless Commun.*, vol. 8, no. 7, pp. 3634–3645, 2009.

[28] F. A. Khan, C. Masouros, and T. Ratnarajah, "Interference-driven linear precoding in multiuser MISO downlink cognitive radio network," *IEEE Trans. Vehi. Technol.*, vol. 61, no. 6, pp. 2531–2543, 2012.

[29] A. Garcia-Rodriguez and C. Masouros, "Power-efficient tomlinson-harashima precoding for the downlink of multi-user MISO systems," *IEEE Trans. Commun.*, vol. 62, no. 6, pp. 1884–1896, 2014.

[30] C. Masouros, M. Sellathurai, and T. Ratnarajah, "Maximizing energy efficiency in the vector precoded MU-MISO downlink by selective perturbation," *IEEE Trans. Wireless Commun.*, vol. 13, no. 9, pp. 4974–4984, 2014.

[31] A. Li, F. Liu, C. Masouros, Y. Li, and B. Vucetic, "Interference exploitation 1-bit massive MIMO precoding: A partial branch-and-bound solution with near-optimal performance," *IEEE Trans. Wireless Commun.*, vol. 19, no. 5, pp. 3474–3489, 2020.

[32] F. Liu, C. Masouros, A. Li, T. Ratnarajah, and J. Zhou, "MIMO radar and cellular coexistence: A power-efficient approach enabled by interference exploitation," *IEEE Trans. Signal Process.*, vol. 66, no. 14, pp. 3681–3695, 2018.

[33] A. Haqiqatnejad, F. Kayhan, and B. Ottersten, "Robust design of power minimizing symbol-level precoder under channel uncertainty," in *2018 IEEE GLOBECOM*, 2018, pp. 1–6.

[34] ——, "Robust sinr-constrained symbol-level multiuser precoding with imperfect channel knowledge," *IEEE Trans. Signal Process.*, vol. 68, pp. 1837–1852, 2020.

[35] A. Morsali and B. Champagne, "Robust hybrid analog/digital beamforming for uplink massive-mimo with imperfect csi," in *2019 IEEE WCNC*, 2019, pp. 1–6.

[36] S. He, J. Wang, Y. Huang, B. Ottersten, and W. Hong, "Codebook-based hybrid precoding for millimeter wave multiuser systems," *IEEE Trans. Signal Process.*, vol. 65, no. 20, pp. 5289–5304, Oct 2017.

[37] J. Zhang, Y. Huang, J. Wang, X. You, and C. Masouros, "Intelligent interactive beam training for millimeter wave communications," *IEEE Trans. Wireless Commun.*, vol. 20, no. 3, pp. 2034–2048, 2021.

[38] A. Alkhateeb, G. Leus, and R. Heath, "Limited feedback hybrid precoding for multi-user millimeter wave systems," *IEEE Trans. Wireless Commun.*, vol. 14, no. 11, pp. 6481–6494, Nov 2015.

[39] A. Li, C. Masouros, B. Vucetic, Y. Li, and A. L. Swindlehurst, "Interference exploitation precoding for multi-level modulations: Closed-form solutions," *IEEE Trans. Commun.*, vol. 69, no. 1, pp. 291–308, 2021.

[40] A. Li, D. Spano, J. Krivochiza, S. Domouchtsidis, C. G. Tsinos, C. Masouros, S. Chatzinotas, Y. Li, B. Vucetic, and B. Ottersten, "A tutorial on

interference exploitation via symbol-level precoding: Overview, state-of-the-art and future directions," *IEEE Communications Surveys Tutorials*, vol. 22, no. 2, pp. 796–839, 2020.
[41] K. I. Pedersen, P. E. Mogensen, and B. H. Fleury, "A stochastic model of the temporal and azimuthal dispersion seen at the base station in outdoor propagation environments," *IEEE Trans. Veh. Technol.*, vol. 49, no. 2, pp. 437–447, 2000.
[42] T. Lattimore and C. Szepesvri, *Bandit Algorithms*. Cambridge University Press, 2020.
[43] C. Blundell, J. Cornebise, K. Kavukcuoglu, and D. Wierstra, "Weight uncertainty in neural networks," in *International Conference on Machine (ICML)*, 2015, pp. 1613–1622.
[44] K. P. Murphy, *Machine learning: a probabilistic perspective*. MIT press, 2012.

Jianjun Zhang (S'16-M'18) received the M.S. degree from Nanjing University of Aeronautics and Astronautics, Nanjing, China, in 2014, and the Ph.D. degree from Southeast University, Nanjing, China, in 2018. He is currently a Research Fellow of the electrical and electronics engineering with University College London (UCL), U.K. He was the recipient of the Best Paper Award in the IEEE Globecom 2019. His current research interests include machine learning and optimization, intelligent communications, and probability theory and its applications.

Christos Masouros (M'06-SM'14) received the Diploma degree in Electrical and Computer Engineering from the University of Patras, Greece, in 2004, and MSc by research and PhD in Electrical and Electronic Engineering from the University of Manchester, UK in 2006 and 2009 respectively. In 2008 he was a research intern at Philips Research Labs, UK. Between 2009-2010 he was a Research Associate in the University of Manchester and between 2010-2012 a Research Fellow in Queen's University Belfast. In 2012 he joined University College London as a Lecturer. He has held a Royal Academy of Engineering Research Fellowship between 2011-2016.

He is currently a Full Professor in the Information and Communication Engineering research group, Department of Electrical and Electronic Engineering, and affiliated with the Institute for Communications and Connected Systems, University College London. His research interests lie in the field of wireless communications and signal processing with particular focus on Green Communications, Large Scale Antenna Systems, Communications and Radar Co-existence, interference mitigation techniques for MIMO and multi-carrier communications. He was the recipient of the Best Paper Awards in the IEEE Globecom 2015 and IEEE WCNC 2019 conferences, and has been recognized as an Exemplary Editor for the IEEE Communications Letters, and as an Exemplary Reviewer for the IEEE Transactions on Communications. He is an Editor for IEEE Transactions on Communications, IEEE Transactions on Wireless Communications, the IEEE Open Journal of Signal Processing, and Editor-at-Large for IEEE Open Journal of the Communications Society. He has been an Associate Editor for IEEE Communications Letters, and a Guest Editor for IEEE Journal on Selected Topics in Signal Processing issues "Exploiting Interference towards Energy Efficient and Secure Wireless Communications", "Hybrid Analog / Digital Signal Processing for Hardware-Efficient Large Scale Antenna Arrays" and "Joint Communication and Radar Sensing for Emerging Applications". He is currently an elected member of the EURASIP SAT Committee on Signal Processing for Communications and Networking.